

1 **Fungal taste for minerals: the ectomycorrhizal fungus *Paxillus involutus* triggers specific genes**  
2 **when extracting potassium from different silicates**

3  
4 Pinzari F.<sup>1,2,\*</sup>, Jungblut A.D.<sup>1</sup>, Cuadros J.<sup>3</sup>

5  
6 <sup>1</sup> Life Sciences Department, Natural History Museum, Cromwell Road, SW7 5BD London, UK

7  
8 <sup>2</sup> Council of National Research of Italy (CNR), Institute for Biological Systems (IBS), Monterotondo  
9 (Rome), Italy.

10  
11 <sup>3</sup> Earth Sciences Department, Natural History Museum, Cromwell Road, SW7 5BD London, UK

12  
13 **Corresponding Author:** Flavia Pinzari, Life Sciences Department, Natural History Museum,  
14 Cromwell Road, SW7 5BD, United Kingdom, email: [f.pinzari@nhm.ac.uk](mailto:f.pinzari@nhm.ac.uk)

15  
16 **Running title:** Transcriptomic response of ectomycorrhiza to potassium mining

17  
18 **Abstract**

19 Silicates make up about 90% of the Earth's crust and constitute the main source of mineral nutrients  
20 for microorganisms and plants. Fungi can actively weather silicates to extract nutrients. However, it  
21 is unclear whether they are able to obtain the same amounts of nutrients and use the same mechanisms  
22 when tapping into different mineral sources. We performed a microcosm experiment using the  
23 ectomycorrhizal basidiomycetes *Paxillus involutus* and the silicates K-vermiculite, muscovite and  
24 phlogopite as only potassium sources, as they show a different resistance for the removal of K cations  
25 from the mineral structure. A combination of transcriptomic, elemental and SEM analyses showed  
26 that different minerals stimulated specific weathering mechanisms and led to a change in fungal genes  
27 expression. The differential expression of the fungal genes generated alternative chemical attacks on  
28 the minerals, resulting in a tailored dissolution and selective uptake of chemical elements according  
29 to the leachability of K from the silicate mineral. The K uptake capacity of the fungus was highest  
30 with vermiculite in comparison to growth on phlogopite and muscovite. The findings provide new  
31 insights into fungal-mineral interactions that will help to interpret key processes for the homeostasis  
32 of soil environments.

33  
34 **Keywords**

35 Fungi, mineral weathering, *Paxillus involutus*, potassium, RNAseq, silicates.

36  
37 **1. Introduction**

38 Weathering of silicates by fungi is an important process in soil formation and chemical evolution of  
39 rocks [1-3]. The ability to dissolve minerals applies to many fungi and in particular to mycorrhizal  
40 fungi, which form mutual symbiotic associations with the plant root system and are able to increase  
41 the dissolution and transformation of silicate minerals while extracting phosphorus (P), potassium  
42 (K), calcium (Ca), magnesium (Mg) and iron (Fe), especially under nutrient limitations [2]. The study  
43 of the genomes of ectomycorrhizal fungi and their transcripts have shown how fungi evolved complex  
44 mechanisms for the assimilation and exchange of carbon (C), P and nitrogen-based compounds [4].  
45 However, metal nutrients have received much less attention, and their biogeochemical routes are  
46 almost unknown [2]. Free-living and mycorrhizal fungi can use a range of mineral dissolution  
47 mechanisms, including acidification of the microenvironment via excretion of protons, phosphoric  
48 acid, organic acids, and carbon dioxide (CO<sub>2</sub>) [5-7]. Fungi also use the production of extracellular  
49 polymeric substances to adsorb and accumulate cations and decrease the saturation for those elements  
50 [8]. Exudation of organic complex-forming molecules [8-9] is as well an essential mechanism for the  
51 modification of water chemistry (e.g., concentrating salts) and viscosity within biofilms that increases

52 water reactivity with the mineral surface [10]. In addition to multiple mechanisms, there also seem to  
53 be different intensities of mineral weathering by fungi [11]. The production of oxalic acid by a fungus,  
54 for example, is modulated according to the type of mineral it comes into contact [12]. It is also known  
55 that there are genes that can be associated with specific weathering mechanisms and that these can be  
56 regulated by the depletion of certain nutrients from the culturing media [13]. What is unclear is  
57 whether, in light of the different structural ways in which nutrients may be part of the mineralogy of  
58 silicates, the fungi not only are able to modulate the intensity of weathering but also to implement  
59 different functional strategies. The ability of fungi to change the metabolic strategy depending on the  
60 type of mineral from which they derive nutrients would have implications for both the ecology and  
61 evolution of fungi and fungi-plant systems [6, 14]. Fungal-derived chemical equilibria in the  
62 biosphere would vary based on gene expression mechanisms and regulatory processes whose control  
63 would disclose new frontiers in agriculture and soil management. In fact, a better understanding of  
64 the regulation of weathering processes by fungi could improve predictions of ecosystem functions  
65 [15- 16]. An active fungal regulation in silicates weathering would also impact Earth system models  
66 and provide new variables to the global C cycle [17-19].

67  
68 This study tested the hypothesis that fungi would show distinct mechanisms of attack and differential  
69 gene expression profiles when grown on specific minerals to obtain limiting nutrients such as K. The  
70 fungus *Paxillus involutus* was selected for the experiments as it is a Basidiomycetes of global  
71 significance [20]. It can form mycorrhizae with many species of trees [21] but is capable also of  
72 growing in axenic culture [22] and can weather minerals [12, 23-25]. *P. involutus* was grown in  
73 microcosm experiments under three different conditions where the only sources of K were the  
74 minerals phlogopite, K-vermiculite and muscovite, and compared with a positive control with K  
75 available in the media and a negative control without any K. These silicates have similar metal  
76 nutrient contents but have different degrees of weatherability, which could trigger a specific fungal  
77 strategy to obtain nutrients and reveal a differential genetic expression. The growth and response of  
78 the fungi were evaluated using RNAseq-based differential gene expression. The mycelium was  
79 analysed to evaluate the uptake of nutrients using inductively coupled plasma mass spectroscopy  
80 (ICP-MS), and the minerals were analysed to detect traces of weathering and patterns of interaction  
81 with the fungal hyphae by means of scanning electron microscopy (SEM).

## 82 83 **2. Materials and Methods**

### 84 85 **2.1 Fungal material and experimental set-up**

86 Cultures of *P. involutus* (Batsch) Fr. (strain ATCC 200175, [www.atcc.org](http://www.atcc.org)) (Basidiomycota,  
87 Boletales) were reactivated and maintained aseptically on Modified Melin–Norkrans (MMN) agar  
88 (Supplementary Materials S1). The purity and identity of *P.involutus* ATCC 200175 strain was  
89 verified by Sanger sequencing (Supplementary Materials S2). The microcosms were prepared  
90 according to Wei et al. [26] with some modifications (Supplementary Materials S3). Three different  
91 minerals with decreasing level of K leachability were used: muscovite, phlogopite, K-vermiculite.  
92 Their structural formulas are specified in Supplementary Materials S4. All cultures were kept in the  
93 dark at 25°C throughout the experiment. The microcosms were incubated for 21 days. Ten biological  
94 replicates from each experiment were used for RNA extraction, five from each experiment were  
95 dismantled and used for ICP-MS analysis, and the corresponding minerals were used in SEM  
96 analysis. After the experiments, fungal biomass was determined by weight using five microcosms  
97 from each experiment (dry weight, 50°C, 48 h). The pH of the agar was measured at the beginning  
98 and the end of the experiments (Electrode n.662-1164, VWR International Ltd, Leicestershire, U.K.).  
99

### 100 **2.2. Microscopic and chemical analysis of fungal biomass and minerals**

101 Mineral samples were analysed before and after the experiment using SEM as described in  
102 Supplementary Materials S5. Groups of five replicates from each experiment were used to analyse

103 sodium (Na), Mg, aluminium (Al), Fe, P, K, and Ca in the fungal mycelium by digestion and analysis  
104 by ICP-MS (Agilent Technologies 7700), as described in Supplementary Materials S6.

105

### 106 **2.3 RNA extraction and libraries preparation**

107 At the end of the experiment, fungal biomass was removed from the cellophane membrane and  
108 ground into a powder in liquid nitrogen. mRNA was extracted using the RNAeasy® PlantMini Kit  
109 (Qiagen, Manchester, U.K.) and libraries prepared using TruSeq Stranded mRNA Kit (Illumina,  
110 Cambridge, UK) (Supplementary Materials S7 and 8). Libraries (5 biological replicates for each  
111 experiment, for a total of 25 samples) were sequenced with Illumina NovaSeq 6000 (2 x 100 bp read-  
112 length) by the CeGAT Company (Germany).

113

### 114 **2.4 Bioinformatic analysis**

115 Full details on the sequence processing are provided in Supplementary Materials S9. Trimmed reads  
116 were aligned to the *Paxillus involutus* reference genome (GCA\_000827475.1) using STAR (v2.5.2b)  
117 [27]. A count table was created using the HTSeq package [28] implemented in OmicBox (version  
118 1.2.4) [29-30]. EdgeR version 2.12 [ref. 31] was used to perform pairwise differential expression  
119 analysis (DEA) between pairs of experimental conditions (5 replicates per experimental condition).  
120 Functional annotation of differentially expressed genes (DEGs) was based on *P.involutus* annotation  
121 from the EnsemblFungi server (<http://fungi.ensembl.org>) with assembly accession number  
122 GCA\_000827475.1 [ref. 21], and by using the BLASTx algorithm within OmicsBox version 1.2.4  
123 (BioBam) [29-30]. Functional annotation of sequences was further achieved using InterProScan [29-  
124 30, 31] and EggNOG-mapper [32]. Gene Set Enrichment Analysis (GSEA) was used to determine  
125 whether an *a priori* defined set of genes showed statistically significant, concordant differences  
126 between two biological states [34]. The normalised enrichment score (NES) was used to compare  
127 analysis results across gene sets. The false discovery rate (FDR), was used as an estimate of the  
128 probability that a gene set with a given NES represented a false positive finding. FDR cut-off was  
129 fixed at 5%.

130

## 131 **3. Results**

### 132 **3.1 Fungal growth**

133 *P. involutus* mycelium grew in all experiments showing good replicability of the in-vitro system  
134 utilised (Fig. S1). The pH of the agar decreased in all the experiments from its initial value of 4.7.  
135 Table S1 shows the pH values in the five experiments at the end of the incubation, with a higher pH  
136 in the positive control (Cp) than in the microcosms with the minerals. The pH values in the treatments  
137 with minerals were significantly different from the positive control, whereas the pH values in the  
138 negative control (Cm) were not significantly different from the positive control or the experiments  
139 with the minerals. The comparison of the fungal biomass content obtained in the five experiments is  
140 shown in Table S2. The wet fungal biomass was significantly higher in the positive control, followed  
141 by the experimental treatment with phlogopite, while significantly lower values were measured in the  
142 K-vermiculite, muscovite and negative control experiments.

143

### 144 **3.2 Fungal weathering of minerals: ICP-MS results**

145 The fungus absorbed more K from K-vermiculite than from the other two minerals (Table 1). There  
146 was a trend indicating a slightly higher concentration of K in experiments run with phlogopite than  
147 muscovite (Table 1), but the K content of mycelium grown in the presence of muscovite and  
148 phlogopite was not significantly different from that recorded in the negative control. Table 2 shows  
149 the Pearson correlation coefficients (*r*) calculated between the mycelial concentrations of the  
150 elements. The coefficient values showed that the absorption of K was positively correlated with P,  
151 Ca and Mg, while it was negatively correlated with the absorption of Na. Moreover, Fe and Al showed  
152 a strong positive correlation ( $r=0.99$ ).

153

### 154 **3.3 Scanning Electron Microscopy of mineral surfaces**

155 The SEM imaging showed that the three minerals were altered by the growth of the fungus during  
156 the microcosm experiments. Comparing SEM images of minerals before and after the experiments  
157 suggested that *P. involutus* when forced to grow under limited availability of K, produced different  
158 effects in each silicate mineral. In muscovite, the surface of the crystal appeared eroded and uneven  
159 (Fig. 1A). At higher magnification, alterations were observed at the contours of the fungal hyphae  
160 consisting in the localised removal of surface layers of the mineral (Fig. 1B). In phlogopite, large  
161 portions of mineral layers were removed (Fig. 1C). In the high-resolution images, the surface of the  
162 phlogopite crystals was fragmented and furrowed, and characteristic depositions arranged in small  
163 regular clusters were observed between the cracks (Fig. 1D). Fungal mycelium appeared singularly  
164 adherent to the crystal when grown on the K-vermiculite. Here, forms of surface erosion were also  
165 visible at low magnification suggesting that the fungus exerted a mechanical action (Fig. 1E).  
166 However, the waxy consistency of the superficial layer of K-vermiculite, at times excavated and  
167 raised to form small accumulations of material, suggests that a chemical action also took place to  
168 make an initially intact crystalline structure malleable. High magnification images of K-vermiculite  
169 surface show some hyphae flattened and others filled with precipitated material (Fig. 1F).

### 171 **3.4 Differential expression of *P. involutus* during K weathering on K-vermiculite, muscovite and 172 phlogopite minerals.**

173 The transcriptome sequencing yielded 966.96 million reads, with a total number of bases (in Gb) of  
174 194.89, an average GC content of trimmed FASTQ reads (average of all samples) of 53.0% to 54.0%  
175 and a Q30 quality score threshold value between 91.3% and 93.07% (Table S3). Multidimensional  
176 scaling analysis (MDS) (Fig. 2) [35] was performed to evaluate the dissimilarity between  
177 transcriptomes of *P. involutus* obtained in response to its growth on K-vermiculite, phlogopite and  
178 muscovite and in comparison to the negative and positive controls. In the two-dimensional scatterplot  
179 (Fig. 2) the distances represent the log<sub>2</sub> fold change (log<sub>2</sub> FC) between samples. The transcriptomes  
180 obtained with minerals were different from the positive control. The transcriptome from the K-  
181 vermiculite microcosm showed a high similarity between replicates and grouped separately from all  
182 the other experiments. The transcriptomes from phlogopite, muscovite and the negative control  
183 overlapped and showed a general higher variability compared to positive control and K-vermiculite  
184 treatment.

185  
186 From the heatmap (Fig. 3) emerges that there are two significant clusters of genes with distinct  
187 regulation for the positive and negative controls. The fungus in the presence of K-vermiculite showed  
188 a gene expression partially similar to the positive control. With muscovite and phlogopite the gene  
189 expression was similar to the negative control. The number of genes differentially expressed by the  
190 fungus in each comparison are shown in Table 3. Overall, the number of genes differentially  
191 expressed between the experiments with the minerals and the negative control is lower than the  
192 number of genes obtained in the contrasts against the positive control. The similarity between the  
193 condition of K deprivation and that of bioavailability conditioned by the mineral source is also shown  
194 by the Volcano plots that display both the genes differentially expressed (FDR < 0.05) and those that  
195 did not show a change in their expression level between contrasting conditions (Figure S2). The  
196 number of significantly up and down-regulated genes (FDR < 0.05) between the experiments and  
197 controls is summarised in Table 3. In the pairwise comparison between transcriptomes of *P. involutus*  
198 grown on the three minerals, and the negative control, the number of differentially expressed genes  
199 decreases from K-vermiculite (439) to phlogopite (47) and muscovite (29). There were very few  
200 DEGs between muscovite and negative control, which indicates that the physiological state of the  
201 fungus in the presence of muscovite was similar to being under the condition of K deprivation.

202  
203 Fig. 4 and Supplementary Spreadsheet 1 show the genes that the fungus either triggered or repressed  
204 at the presence of the three minerals and the positive control, compared to the negative control based

205 on FDR values and log<sub>2</sub>FC scores. The differential expression between positive and negative control  
206 identified marked differences between the condition of total bioavailability of K and its unavailability,  
207 with genes showing up to 6 log<sub>2</sub>FC values. However, the top genes were assigned as hypothetical  
208 proteins without associated specific function.  
209

### 210 **3.5 Gene set enrichment analysis (GSEA)**

211 The genes that were identified as differentially expressed between pairs of treatments were grouped  
212 by their involvement in biological processes, molecular functions and cellular compartments. In Fig.  
213 5 and Supplementary Spreadsheet 2 are shown the normalised enrichment score values (NES)  
214 obtained for comparisons between the experiments in which the fungus grew in the presence of the  
215 three minerals (V, P and M) compared to the negative control condition (Cm). Among the molecular  
216 functions stimulated in the experiments with phlogopite there were carboxylic-acid metabolic process  
217 (GO:0019752), organic-acid metabolic process (GO:0006082), oxoacid metabolic process  
218 (GO:0043436) and lipid metabolic process (GO:0006629). The molecular functions stimulated in the  
219 case of muscovite were different and significantly fewer, compared to the other two minerals. The  
220 only molecular functions overexpressed in *P.involutus* when incubated with muscovite were  
221 monooxygenase activity (GO:0004497) and oxidoreductase activity (GO:0016705-MF).  
222 Interestingly, the biological processes that were under-expressed (compared to the negative control  
223 condition) were response to heat (GO:0009408), cellular response to heat (GO:0034605) and  
224 ribonucleoprotein complex subunit organisation (GO:0071826). There were also differences  
225 observed in the gene assignment for the fungus grown with K-vermiculite as the only source of K. In  
226 this condition, both molecular functions and biological processes were associated with the  
227 cytoskeleton, and significant overexpression of gene sets related to cytoskeletal protein binding  
228 (GO:0008092) and cytoskeleton organisation (GO:0007010). Moreover, with K-vermiculite,  
229 catabolic process (GO:0009056), vesicle-mediated transport (GO:0016192), and cellular response to  
230 stimulus (GO:0051716 i.e. processes resulting in a change in state or activity of a cell) were also  
231 overexpressed.  
232

## 233 **4. Discussion**

234 The present study confirmed that *Paxillus involutus* is able to weather K from silicates such as K-  
235 vermiculite, muscovite, and phlogopite, but we also showed for the first time that the gene expression  
236 patterns and metabolic response differed according to K leachability from different types of silicate  
237 minerals. Differences in chemical and physical attack by the fungus on the three minerals were also  
238 documented by chemical and imaging analyses.  
239

### 240 **4.1 Effects on pH and uptake of K and other mineral nutrients**

241 The pH of the agar under the mycelium decreased significantly in all K-depletion treatments, which  
242 is likely due to secretion of acids by the fungus in response to either the absence of K or the presence  
243 of K containing minerals in the agar. This stimulation of acid secretion appeared stronger in the  
244 presence of minerals than in the negative control, which reinforces the idea that it is not the absence  
245 of K, but the presence of minerals containing it, that stimulated the secretion of acids into the culture  
246 medium. K concentration in the mycelium was negatively correlated with Na concentration, but  
247 positively correlated with P. There was no clear correlation observed between Mg and Ca. The  
248 negative correlation of K with Na was likely due to the use of Na as a substitute for K by the fungus.  
249 This can be explained by K being the primary inorganic cation in the fungal cell cytoplasm and an  
250 essential macro-element that is accumulated against a transmembrane concentration gradient. If the  
251 K deficiency occurs in the presence of Na, fungal cells can take Na<sup>+</sup> instead of H<sup>+</sup> as a substitute for  
252 the missing K [36]. While fungi can utilise Na to grow in the absence of K, Na is also a toxic element  
253 in excessive quantities [37]. Thus, the recorded changes in gene expression that depended on K  
254 limitation could have been linked to functional modifications needed at membrane level to assimilate  
255 Na instead of K, and mechanisms to react to Na toxicity [38].

256  
257  
258  
259  
260  
261  
262  
263  
264  
265  
266  
267  
268  
269  
270  
271  
272  
273  
274  
275  
276  
277  
278  
279  
280  
281  
282  
283  
284  
285  
286  
287  
288  
289  
290  
291  
292  
293  
294  
295  
296  
297  
298  
299  
300  
301  
302  
303  
304  
305  
306

We also observed a positive correlation of K and P, which could be due either to differential P uptake, or to differential P excretion. The findings agree with previous studies, where a strong correlation between P and K cellular levels was observed for the ectomycorrhizal fungus *Hebeloma cylindrosporum* [39]. Jentschke et al. [40] found that the fungus *P. involutus* translocated K and Mg to Norway spruce plants, with the translocation of these elements depending on their coupling with P uptake during the process. Our findings also suggest that K was one of the major counter-ions of polyphosphate (polyP) granules, especially of soluble polyP short-chains, mainly located in fungal vacuoles [41]. K and P have been shown to be located in the same vacuolar fungal compartments of *P. involutus* [42-43]. P uptake and polyphosphates synthesis and accumulation could result in the accumulation of a high negative charge in the cell, which results in the activation of cation import mechanism for maintaining overall cellular charge neutrality. Therefore, K is both an element directly involved in fungal nutrition, but also a component necessary for cell homeostasis and efficient uptake and storage of inorganic phosphate. Although the fungus grew in K-depleted experiments and P was not limiting, less P was assimilated than in the positive control. This indicates that the limitation in the bioavailability of K could have affected P assimilation.

The SEM imaging allowed to document visible effects of metabolic action by the fungus on minerals at microscale level. The K extraction led to the formation of furrows, cracks, swelling, erosions and bio-precipitation of material on crystals. Some of the effects are due to the production of organic acids, the adhesion of hyphae and leaching of elements other than K. For example, the mycelium grown in the presence of phlogopite showed significantly higher assimilation of Fe and Al than the other experiments. Ectomycorrhizal fungi can assimilate Fe [44] and are also capable of absorbing Al [45]. Similarly, Bonneville et al. [44] showed that *Paxillus involutus* could oxidise Fe(II) to Fe(III) in biotite, increasing with this process the mineral weathering. The authors suggested that Fe(II) oxidation induces the loss of the newly formed Fe(III) from the octahedral sheets and formation of amorphous Fe oxy-hydroxides within the silicate layers, which induces volume increase, strain in the biotite lattice and the formation of fractures.

#### 4.2 Differential gene expression of *P. involutus* as a response to growth on silicates with variable K leachability

The gene expression profiles by *P. involutus* were distinct for mycelium grown on K-vermiculite in comparison to muscovite and phlogopite as well as to controls. The muscovite and phlogopite experiments had similar profiles and overlapped with the negative control. The differential expression of genes matched to the concentration of K found in the mycelium after the experiments, and there was a positive relationship between the accessibility of the element and its absorption by the fungus. This suggested the fungus modulated the gene expression according to both the amount of K that it was able to assimilate from the silicates but also reflected the strength with which the three minerals retained the cation. As the three minerals showed some variation in the weathering of other elements such as Fe, Mg, Na and Al, the gene expression profile might also be affected by other factors than leachability of K from the respective mineral, including toxicity of released metals, and solubility of the other cations in the growth environment [46-47].

In the presence of K-vermiculite, the fungus was able to derive the K by its displacement from the interlayer sites of vermiculite by other cations in the medium, which is an exchange mechanism similar to how fungi obtain minerals in soil environments [48]. This suggests that the fungus was not subjected to the same level of K deprivation as with the other two minerals. However, it still had to activate different mechanisms for the assimilation of K than under condition of its unlimited bioavailability (in positive control). In the case of muscovite, which is the mineral most strongly retaining K, the gene expression profiles suggested a response similar to growth in the absence of K. There were only 21 genes up- and 8 down-regulated by the fungus in the presence muscovite in

307 comparison to the negative control, moreover, only a few of these were found to be differentially  
308 expressed for more than 2 logFC. In terms of K effectively being assimilated by the fungus, the  
309 difference corresponds to about one microgram per dry gram of mycelium. These few genes are  
310 therefore those that separate the condition of total K depletion from that of a minimum bioavailability.  
311 The most differentially expressed genes (downregulated more than 2 logFC in the presence of  
312 muscovite, compared to negative control) were a glycoside hydrolase family 79 protein from the  
313 membrane (PAXINDRAFT\_153975, GO:0016020), a hypothetical protein associated to the nucleus,  
314 involved in regulation of transcription by RNA polymerase II and with DNA-binding transcription  
315 factor activity (PAXINDRAFT\_176752, P:GO:0006357; F:GO:0000981; F:GO:0008270) and an  
316 RnaseH-domain-containing protein, with RNA phosphodiester bond hydrolytic function, binding  
317 nucleic acids (PAXINDRAFT\_91567, P:GO:0090502; F:GO:0003676; F:GO:0004523). The  
318 glycoside hydrolase family 79 protein includes endo-beta-N-glucuronidase (EC 3.2.1.31) and  
319 enzymes with  $\beta$ -glucanase activity, that in fungi are thought to be necessary in morphogenetic events  
320 that require controlled hydrolysis of the cell wall [49].

321 Comparison of positive and negative control conditions showed that more genes were up regulated  
322 under unlimited K bioavailability than under stress conditions of K depletion. Which corresponds to  
323 a large down-regulation of genes in the negative control. This can be read as a response to stress with  
324 the deactivation of functions in order to overcome the nutrients limitation. Still, a significant down  
325 regulation of genes in the positive control microcosms experiments was also observed, indicating the  
326 existence of a number of mechanisms that have evolved to respond to the absence of K in the  
327 environment. However, the fungus still grew under K-depleted conditions as the dry weight of the  
328 mycelium in the negative control was not significantly different to biomass in the positive control.  
329 This could be due to the increased uptake of Na to replace K as cation, as Na content of the mycelium  
330 in the negative control was at least seven times that of the positive control. The change in gene  
331 expression triggered by K limitation could have therefore been linked to functional modifications  
332 needed at membrane level to assimilate Na instead of K, and to limit any toxic effects by the increased  
333 uptake of Na in to the cells. Similar mechanisms of reaction of *P. involutus* to limiting nutritional  
334 conditions have been observed by Papanikolaou et al. [50] who showed that inorganic P starvation  
335 induces in the fungus expression of newly identified putative high-affinity Pi transporter genes, while  
336 reducing the expression of putative organic acid transporters.

#### 337 338 4.3 Differences in functional genes and processes for K leaching from silicates

339 Phlogopite, K-vermiculite and muscovite led to distinct transcriptional responses in the fungus,  
340 suggesting some mechanism by the fungus to sense and respond to its mineral surroundings. Gene  
341 expression of the fungus in the presence of K-vermiculite compared to the condition of total K  
342 depletion highlighted the overexpression of genes that interact with cytoskeleton components which  
343 have a role in the assembly or disassembly of cytoskeletal structures such as actin. They are also  
344 involved in vesicle-mediated transport, and suggests that adhesion mechanisms could have had a role  
345 in K uptake. Indeed, fungi, in addition to dissolving the minerals with the production of acidic  
346 substances, have shown in some studies to carry out physical attacks on minerals through hyphal  
347 adhesion. It has been shown for example that the release of K was enhanced by a factor of 3-4 by  
348 direct contact between K-feldspar and illite surfaces and the fungus [51]. Attachment of fungi to the  
349 mineral surfaces has also been shown to cause a more efficient release of elements from biotite [52-  
350 53]. Physical mechanisms of action may be therefore particularly efficient for some cations such K.

351  
352 Phlogopite triggered the overexpression of genes associated with the chemical reactions and pathways  
353 involving carboxylic acids, organic acids and also oxoacid metabolic process. An oxoacid is a  
354 compound which contains oxygen and which produces a conjugate base by loss of positive hydrogen  
355 ion(s). Many organic acids, like carboxylic acids, are oxoacids. Van Schöll et al. [25] showed how  
356 ectomycorrhizal fungi lacking mineral nutrients like P, Mg, and K might modify the composition of  
357 organic acids they exude. In other fungi, oxalate exudation was found to be higher when the mycelium

358 was in contact with rock grains containing K [54]. Furthermore, the biological processes that were  
359 stimulated by phlogopite involved the hydrolytic activity linked to P-containing anhydrides for the  
360 catalytic reaction that produces nucleoside diphosphate and a phosphate from nucleoside  
361 triphosphate. There are the adenosine triphosphatases (ATPases) that generate electrical and chemical  
362 ion gradients across membranes and transporters for a wide range of solutes across membranes.  
363 Another gene up-regulated by the fungus in the presence of phlogopite, compared to the negative  
364 control, is a phosphoglycerate mutase-like protein, which was annotated as an integral component of  
365 the plasma membrane. The top up-regulated gene in K-vermiculite was also a hypothetical protein  
366 that is located in the membrane and is involved in ATP-coupled electron transport and electron  
367 transfer activity. This highlights the involvement in transport mechanisms during leaching and uptake  
368 of K from silicates.

369  
370 Monoxygenase and oxidoreductase activities were the only molecular functions significantly  
371 overexpressed as gene sets in the presence of muscovite. Fungi produce heme-containing peroxidases  
372 and peroxygenases, flavin-containing oxidases, and different copper-containing oxidoreductases  
373 [55]. Moreover, in some basidiomycetes unspecific peroxygenases can catalyse a variety of  
374 monoxygenation reactions with H<sub>2</sub>O<sub>2</sub> as the source of oxygen and final electron acceptor. Oxidation  
375 processes are more energy-demanding than acid production, and therefore they might have been used  
376 by the fungus after failure to leach K under acidic conditions, as suggested by the low uptake of K in  
377 the mycelium and the limited uptake of Al, compared to phlogopite, and by the evidence that fungal  
378 weathering of Al from muscovite occur by releasing organic acids [56]. Xiao et al. [57] and Wang et  
379 al. [58] suggested that genes encoding multicopper oxidase have a significant role in the weathering  
380 of K-bearing silicates in *Aspergillus* spp. Our study identified a gene encoding for di-copper centre-  
381 containing protein with oxidoreductase and metal ion binding function as up-regulated by the fungus  
382 grown with muscovite. Wang et al. [59] also showed with an electrochemical experiment that  
383 multicopper oxidases could enhance electrons transfer during fungal weathering of K-bearing  
384 silicates, promoting electron transport at the edge of the minerals.

385  
386 There are four families of putative K transport systems identified in ectomycorrhizal fungi [60]. HAK  
387 and Trk transporters, TOK and SKC channels, the latter representing voltage-dependent K-selective  
388 channels. In particular, Trk transporters are membrane proteins involved in K uptake that are  
389 widespread among fungi [61]. HcTrk1, one member of these transporters that are present in some  
390 ectomycorrhizal fungi [62] was described as a Na<sup>+</sup> /K<sup>+</sup> transporter. However, in *P. involutus* none  
391 of the genes belonging to K transporters (HAK and Trk transporters, or to TOK and SKC channels)  
392 were significantly up-regulated in the microcosms with the minerals compared to the negative control.  
393 In contrast, several genes associated with transport systems were down-regulated in the mycelia  
394 grown with K-vermiculite compared to negative control, including a P-loop containing nucleoside  
395 triphosphate hydrolase protein associated to ATPase-coupled transmembrane transporter. There was  
396 also a gene down-regulated in the muscovite experiment that is associated with a general substrate  
397 transmembrane transporter (major facilitator superfamily MFS), and an integral component of the  
398 plasma membrane. The MFS are membrane proteins that import and export target substrates such as  
399 metabolites, oligosaccharides, amino acids and oxyanions. They utilise the electrochemical gradient  
400 of the target substrate (uniporter), or act as a co-transporter where transport is coupled to the  
401 movement of a second substrate.

402  
403 The presented study is based on laboratory experiments, however the fungus *P. involutus* is abundant  
404 in the environment and forms mycorrhizae with many tree species. Many soil environments can be  
405 cation-poor and therefore the ability of *P. involutus* to access K from minerals would give an  
406 ecological advantage. Therefore, the fungi might have even evolved specific cellular and metabolic  
407 mechanisms [48, 63]. An adaptation of the fungi to low K conditions could help to explain the  
408 observed down regulation of many genes in the positive control microcosms experiments. The down



409 regulated genes under unlimited K conditions were predicted to be linked to fundamental fungal  
410 biological processes, such as "translation", "carbohydrate metabolic processes" or "ribosome  
411 biogenesis". A large set of genes (over 200) associated to the "mitochondrion" cellular components  
412 were also significantly down-regulated. This suggest that the fungi might had a lower energy  
413 expenditure and cellular activity in the presence readily bioavailable K.

414

## 415 **5. Conclusions**

416 The geo-biological cycles are governed by complex interactions and feedback mechanisms between  
417 living organisms and rocks. Filamentous fungi play a key role as they collaborate symbiotically with  
418 plants, decompose and recycle organic matter and extract nutrients from minerals. One of the  
419 fundamental nutrients for growth is K, and the global transcriptome analysis showed that *Paxillus*  
420 *involutus* could switch on or off different genes and metabolic pathways depending on the minerals  
421 from which it is forced to obtain K. The differential expression of the fungal genes generated  
422 alternative chemical attacks on the minerals, resulting in a tailored dissolution and selective uptake  
423 of chemical elements. The fungus also showed an excellent exchange capacity with K-vermiculite,  
424 which appeared to create a different condition from that represented by phlogopite and muscovite.  
425 Understanding the strategy deployed by microorganisms to obtain mineral nutrients under different  
426 conditions provides new insights for interpreting the processes on which biodiversity and the  
427 homeostasis of soil environments depend.

428

## 429 **6. Supplementary material**

430

431 **Supplementary Methods:** S1, MMN complete medium composition; S2, Confirmation of purity and  
432 identity of *P. involutus* strain; S3, Microcosm experiment; S4, Mineral substrates used for fungal  
433 weathering experiments; S5, SEM of mineral surfaces; S6, ICP-MS of mycelium; S7, RNA  
434 extraction; S8, Library preparation using TruSeq Stranded mRNA (Illumina) kit; S9, Bioinformatic  
435 analysis; S10, Statistical tests.

436 **Supplementary Tables:** Supplementary Table S1, pH of agar under the mycelium; Supplementary  
437 Table S2, Average fungal biomass; Supplementary Table S3, Results of the sequencing of fungal  
438 mRNA.

439 **Supplementary Figures:** Supplementary Figure S1, Diagram showing the setup of the experiment;  
440 Supplementary Figure S2, Volcano plots

441 **Supplementary Spreadsheets:** Supplementary Spreadsheet 1, Excel file containing the list of top up-  
442 regulated and down-regulated genes; Supplementary Spreadsheet 2, Excel file containing the list of  
443 GSEA results.

444

## 445 **Availability of data and material (data transparency)**

446 The datasets generated during and analysed during the current study are available in the Geo  
447 Submission Omnibus (GEO) public database ([geo@ncbi.nlm.nih.gov](http://geo.ncbi.nlm.nih.gov)) with the accession number  
448 GSE158973.

449

## 450 **Acknowledgements**

451 We thank Elena Lugli and Andie Hall for their daily support at the Molecular Laboratory, Emma  
452 Humphreys-Williams for her advice on chemical analyses, Luca Venturini and Matt Clark for helpful  
453 suggestions on bioinformatics solutions, Nathan Kenny for his suggestions on the manuscript, Innes  
454 Clatworthy and Alex Ball for support with SEM-EDS instrumentation.

455

## 456 **Funding**

457 This research was funded by a Newton International Fellowship of the Royal Society to F.P.  
458 (NF170295).

459

## 460 **Conflicts of interest/Competing interests**

461 The authors declare that the research was conducted in the absence of any commercial or financial  
462 relationships that could be construed as a potential conflict of interest.

463

## 464 **Authors' contributions**

465 F.P. conceived the design of the study, conducted molecular analyses, analysed and interpreted  
466 transcriptomic data and wrote the manuscript. A.J. conceived the design of the study, supervised the  
467 molecular and genetic part of project, and wrote the manuscript. J.C. conceived the design of the  
468 study, supervised the geochemical aspects of the project and wrote the manuscript.

469

## 470 **References**

- 471 [1] Hoffland E, Kuyper TW, Wallander H, Plassard C, Gorbushina AA, Haselwandter K, *et al.* The  
472 role of fungi in weathering. *Front Ecol Environ.* 2004; 2: 258–264.
- 473 [2] Cuadros J. Clay minerals interaction with microorganisms: A review. *Clay Miner.* 2017; 52(2):  
474 235-261.
- 475 [3] Fomina M, Skorochod I. Microbial Interaction with Clay Minerals and Its Environmental and  
476 Biotechnological Implications. *Minerals.* 2020; 10(10): 861.
- 477 [4] van der Heijden MGA, Martin FM, Selosse M-A, Sanders IR. Mycorrhizal ecology and evolution:  
478 the past, the present, and the future. *New Phytol.* 2015; 205: 1406–1423.
- 479 [5] Rosling A, Lindahl BD, Taylor AFS, Finlay RD. Mycelial growth and substrate acidification of  
480 ectomycorrhizal fungi in response to different minerals. *FEMS Microbiol Ecol.* 2004; 47(1): 31–  
481 37. [https://doi.org/10.1016/S0168-6496\(03\)00222-8](https://doi.org/10.1016/S0168-6496(03)00222-8).
- 482 [6] Fomina M, Burford EP, Gadd G. Fungal dissolution and transformation of minerals: significance  
483 for nutrient and metal mobility. In: Gadd GM (ed.). *Fungi in Biogeochemical Cycles.* (Cambridge  
484 University Press, Cambridge) (ISBN: 978-0-521-84579-3). 2006. pp 236–266.
- 485 [7] Balogh-Brunstad Z, Kent Keller C, Thomas Dickinson J, Stevens F, Li C, Bormann BT. Biotite  
486 weathering and nutrient uptake by ectomycorrhizal fungus, *Suillus tomentosus*, in liquid-culture  
487 experiments. *Geochim Cosmochim Acta.* 2008; 72: 2601–2618.
- 488 [8] Bray AW, Oelkers EH, Bonneville S, Wolff-Boenisch D, Potts NJ, Fones GR, Benning LG. The  
489 effect of pH, grain size, and organic ligands on biotite weathering rates. *Geochim Cosmochim*  
490 *Acta.* 2015; 164: 127–145.
- 491 [9] Adeyemi AO, Gadd GM. Fungal degradation of calcium-, lead- and silicon-bearing minerals.  
492 *Biometals.* 2005; 18: 269–281.
- 493 [10] Cuadros J, Afsin B, Jadubansa P, Ardakani M, Ascaso C, Wierzchos J. Pathways of volcanic  
494 glass alteration in laboratory experiments through inorganic and microbially-mediated processes.  
495 *Clay Miner.* 2013; 48: 423–445.
- 496 [11] Pinzari F, Cuadros J, Napoli R, Canfora L, Baussà Bardají D. Routes of phlogopite weathering  
497 by three fungal strains. *Fungal Biol.* 2016; 120(12): 1582–1599.
- 498 [12] Schmalenberger A, Duran AL, Bray AW, Bridge J, Bonneville S, Benning LG, *et al.* Oxalate  
499 secretion by ectomycorrhizal *Paxillus involutus* is mineral-specific and controls calcium  
500 weathering from minerals. *Sci Rep;* 2015; 5: 1–14.
- 501 [13] Xiao B, Lian B, Sun L, Shao W. Gene transcription response to weathering of K-bearing minerals  
502 by *Aspergillus fumigatus*. *Chem Geol.* 2012; 306:1–9.
- 503 [14] Naranjo-Ortiz MA, Gabaldón T. Fungal evolution: major ecological adaptations and  
504 evolutionary transitions. *Biol Rev Camb Philos Soc.* 2019; 94(4): 1443–1476.
- 505 [15] Finlay RD, Mahmood S, Rosenstock N, Bolou-Bi EB, Köhler SJ, Fahad Z, *et al.* Reviews and  
506 syntheses: Biological weathering and its consequences at different spatial levels – from nanoscale  
507 to global scale. *Biogeosciences.* 2020; 17: 1507–1533.
- 508 [16] Hu A, Wang J, Sun H, Niu B, Si G, Wang J. *et al.* Mountain biodiversity and ecosystem  
509 functions: interplay between geology and contemporary environments. *ISME J.* 2020; 14: 931–  
510 944. <https://doi.org/10.1038/s41396-019-0574-x>

- 511 [17] Penman DE, Caves Rugenstein JK, Ibarra DE, Winnick MJ. Silicate weathering as a feedback  
512 and forcing in Earth's climate and carbon cycle. *Earth-Science Reviews*. 2020; 209: 103298,  
513 [18] Treseder KK, Lennon JT. Fungal traits that drive ecosystem dynamics on land. *Microbiol Mol*  
514 *Biol Rev*. 2015; 79(2): 243–262.  
515 [19] Zanne A, Abarenkov K, Afkhami M, Aguilar-Trigueros CA, Bates S, Bhatnagar JM, *et al.*  
516 Fungal functional ecology: bringing a trait-based approach to plant-associated fungi. *Biol Rev*.  
517 2020; 95(2): 409–433.  
518 [20] Jargeat P, Chaumeton JP, Navaud O, Vizzini A, Gryta H. The *Paxillus involutus* (Boletales,  
519 Paxillaceae) complex in Europe: genetic diversity and morphological description of the new  
520 species *Paxillus cuprinus*, typification of *P. involutus* s.s., and synthesis of species boundaries.  
521 *Fungal Biol*. 2014; 118(1): 12–31. doi: 10.1016/j.funbio.2013.10.008.  
522 [21] Kohler A, Kuo A, Nagy LG, Morin E, Barry KW, Buscot F, *et al.* Convergent losses of decay  
523 mechanisms and rapid turnover of symbiosis genes in mycorrhizal mutualists. *Nat Genet*. 2015;  
524 47(4): 410–415. doi: 10.1038/ng.3223.  
525 [22] Lapeyrie F, Chilvers GA, Bhém CA. Oxalic acid synthesis by the mycorrhizal fungus *Paxillus*  
526 *involutus* (Batsch EX FR) F.R. *New Phytol*. 1987; 106:139–146.  
527 [23] Smits MM, Bonneville S, Benning LG, Banwart SA, Leake JR. Plant-driven weathering of  
528 apatite – the role of an ectomycorrhizal fungus. *Geobiology*. 2012; 10: 445–456.  
529 [24] Saccone L, Gazze S, Duran A, Leake J, Banwart S, Ragnarsdottir K, *et al.*, High resolution  
530 characterisation of ectomycorrhizal fungal-mineral interactions in axenic microcosm  
531 experiments. *Biogeochemistry*. 2012; 111: 411–425. doi:10.1007/s10533-011-9667-y.  
532 [25] van Schöll L, Smits MM, Hoffland E. Ectomycorrhizal weathering of the soil minerals muscovite  
533 and hornblende. *New Phytol*. 2006; 171(4): 805–813.  
534 [26] Wei Z, Kierans M, Gadd G. A Model Sheet Mineral System to Study Fungal Bioweathering of  
535 Mica. *Geomicrobiol J*. 2012; 29: 323–331.  
536 [27] Dobin A, Davis CA, Schlesinger F, Drenkow J, Zaleski C, Jha S *et al.* STAR: ultrafast universal  
537 RNA-seq aligner. *Bioinformatics*. 2013; 29 (1): 15–21.  
538 [28] Anders S, Pyl PT, Huber W, HTSeq—a Python framework to work with high-throughput  
539 sequencing data. *Bioinformatics*. 2015; 31(2): 166–169.  
540 [29] Conesa A, Götz S, Garcia-Gomez JM, Terol J, Talon M, Robles M. Blast2GO: a universal tool  
541 for annotation, visualisation and analysis in functional genomics research. *Bioinformatics*. 2005;  
542 21: 3674–3676.  
543 [30] Conesa A, Götz S. Blast2GO: A Comprehensive Suite for Functional Analysis in Plant  
544 Genomics. *Int J Plant Genomics*. 2008; 1–13. 2008: 619832. doi: 10.1155/2008/619832.  
545 [31] Robinson MD., McCarthy DJ. and Smyth GK. (2010). edgeR: a Bioconductor package for  
546 differential expression analysis of digital gene expression data. *Bioinformatics* (Oxford, England).  
547 2010; 26(1): 139–140.  
548 [32] Labarga A, Valentin F, Anderson M, Lopez R. Web Services at the European Bioinformatics  
549 Institute, *Nucleic Acids Res*. 2007; 35 (Issue suppl-2): W6–W11.  
550 <https://doi.org/10.1093/nar/gkm291>.  
551 [33] Huerta-Cepas J, Forslund S, Coelho LP, Szklarczyk D, Jensen L, von Mering C, Bork P. Fast  
552 Genome-Wide Functional Annotation through Orthology Assignment by eggNOG-Mapper. *Mol*  
553 *Biol Evol*. 2017; 34. 10.1093/molbev/msx148.  
554 [34] Subramanian A, Tamayo P, Mootha VK, Mukherjee S, Ebert BL, Gillette MA, *et al.* Gene set  
555 enrichment analysis: A knowledge-based approach for interpreting genome-wide expression  
556 profiles. *PNAS*. 2005; 102(43): 15545–15550.  
557 [35] Chen Y, Meltzer PS. Gene Expression Analysis via Multidimensional Scaling. *Current Protocols*  
558 *in Bioinformatics*. 2005; Chapter 7: Unit 7.11. doi: 10.1002/0471250953.bi0711s10.  
559 [36] Rodriguez-Navarro, A. Potassium transport in fungi and plants. *Biochim Biophys Acta*. 1999;  
560 1469 (2000): 1–30.

- 561 [37] Camacho M, Ramos J, Rodríguez-Navarro A. Potassium requirements of *Saccharomyces*  
562 *cerevisiae*. *Curr Microbiol.* 1981; 6: 295–299.
- 563 [38] Gostinčar C, Lenassi M, Gunde-Cimerman N, Plemenitaš A. Fungal adaptation to extremely  
564 high salt concentrations. *Adv Appl Microbiol.* 2011; 77: 71–96.
- 565 [39] Garcia K, Delteil A, Conejero G, Becquer A, Plassard C, Sentenac H, Zimmermann S. Potassium  
566 nutrition of ectomycorrhizal *Pinus pinaster*: overexpression of the *Hebeloma cylindrosporum*  
567 HcTrk1 transporter affects the translocation of both K and P in the host plant. *New Phytol.* 2014;  
568 201: 951–960.
- 569 [40] Jentschke G, Brandes B, Kuhn AJ, Schröder WH, Godbold DL. Interdependence of phosphorus,  
570 nitrogen, potassium and magnesium translocation by the ectomycorrhizal fungus *Paxillus*  
571 *involutus*. *New Phytol.* 2001; 149: 327–337.
- 572 [41] Bücking H, Heyser W. Elemental composition and function of polyphosphates in  
573 ectomycorrhizal fungi — an X-ray microanalytical study. *Mycol Res.* 1999; 103(1): 31–39.
- 574 [42] Orlovich DA, Ashford AE. Polyphosphate granules are an artefact of specimen preparation in  
575 the ectomycorrhizal fungus *Pisolithus tinctorius*. *Protoplasma.* 1993; 173: 91–105.
- 576 [43] Ashford AE, Vesik PA, Orlovich DA, Markovina A-L, Allaway WG. Dispersed polyphosphate  
577 in fungal vacuoles of *Eucalyptus pilularis*/*Pisolithus tinctorius* ectomycorrhizas. *Fungal Genet*  
578 *Biol.* 1999; 28: 21–33.
- 579 [44] Bonneville SC, Bray A, Benning L. Structural Fe(II) Oxidation in Biotite by an Ectomycorrhizal  
580 Fungi Drives Mechanical Forcing. *Environ sci & technol.* 2016; 50(11): 5589–5596.
- 581 [45] Väre H. Aluminium polyphosphate in the ectomycorrhizal fungus *Suillus variegatus* (Fr.) O.  
582 Kunze as revealed by energy dispersive spectrometry. *New Phytol.* 1990; 116: 663–668.
- 583 [46] Gadd GM. Metals, minerals and microbes: geomicrobiology and bioremediation. *Microbiology.*  
584 2010; 156(3): 609–643.
- 585 [47] Illmer P, Buttinger R. Interactions between iron availability, aluminium toxicity and fungal  
586 siderophores. *Biometals.* 2006; 19(4): 367–377.
- 587 [48] Haro R, Benito B. The Role of Soil Fungi in K<sup>+</sup> Plant Nutrition. *Int J Mol Sci.* 2019; 20(13):  
588 3169. doi:10.3390/ijms20133169.
- 589 [49] Dueñas-Santero E, Martín-Cuadrado AB, Fontaine T, Latgé J P, del Rey F, Vázquez de Aldana  
590 C. Characterization of glycoside hydrolase family 5 proteins in *Schizosaccharomyces pombe*.  
591 *Eukaryotic cell.* 2010; 9(11): 1650–1660.
- 592 [50] Paparokidou C, Leake JR, Beerling DJ *et al.* Phosphate availability and ectomycorrhizal  
593 symbiosis with *Pinus sylvestris* have independent effects on the *Paxillus involutus* transcriptome.  
594 *Mycorrhiza.* 2012; 31: 69–83.
- 595 [51] Lian B, Wang B, Pan M, Liu C, Teng HH. Microbial release of potassium from K-bearing  
596 minerals by thermophilic fungus *Aspergillus fumigatus*. *Geochim Cosmochim Acta.* 2008; 72:87–  
597 98.
- 598 [52] Bonneville S, Smits MM, Brown A, Harrington J, Leake JR, Brydson R, Benning LG. Plant-  
599 driven fungal weathering: Early stages of mineral alteration at the nanometer scale. *Geology.*  
600 2009; 37(7): 615–618.
- 601 [53] Ahmed E, Holmström SJM. Microbe-mineral interactions: The impact of surface attachment on  
602 mineral weathering and element selectivity by microorganisms. *Chem Geol.* 2015; 403: 13–23.
- 603 [54] van Hees PA, Rosling A, Essén S, Godbold DL, Jones DL, Finlay RD. Oxalate and ferricrocin  
604 exudation by the extramatrical mycelium of an ectomycorrhizal fungus in symbiosis with *Pinus*  
605 *syvestris*. *New Phytol.* 2006; 169(2): 367–77. doi: 10.1111/j.1469-8137.2005.01600.x.
- 606 [55] Martínez AT, Ruiz-Dueñas FJ, Camarero S, Serrano A, Linde D, Lund H *et al.* Oxidoreductases  
607 on their way to industrial biotransformations. *Biotechnol Adv.* 2017; 35(6); 815–831.
- 608 [56] Song M, Pedruzzi I, Peng Y, Li P, Liu J-F, Yu J. K-Extraction from Muscovite by the Isolated  
609 Fungi. *Geomicrobiol J.* 2015; 32(9): 771–779.
- 610 [57] Xiao L, Sun Q, Lian B. A Global View of Gene Expression of *Aspergillus nidulans* on  
611 Responding to the Deficiency in Soluble Potassium. *Curr Microbiol.* 2016; 72(4): 410–419.

- 612 [58] Wang W, Lian B, Pan L. An RNA-sequencing study of the genes and metabolic pathways  
613 involved in *Aspergillus niger* weathering of potassium feldspar. *Geomicrobiol J.* 2015; 32(8):  
614 689–700.
- 615 [59] Wang W, Sun Q, Lian B. Redox of Fungal Multicopper Oxidase: A Potential Driving Factor for  
616 the Silicate Mineral Weathering, *Geomicrobiol J.* 2018; 35(10): 879–886.
- 617 [60] Garcia K and Zimmermann SD. The role of mycorrhizal associations in plant potassium  
618 nutrition. *Front. Plant Sci.* 2014; 5: 337. doi: 10.3389/fpls.2014.00337
- 619 [61] Benito B, Garciadeblás B, Fraile-Escanciano A *et al.* Potassium and sodium uptake systems in  
620 fungi. The transporter diversity of *Magnaporthe oryzae*. *Fungal Genet Biol.* 2011; 48: 812–822.
- 621 [62] Corratgé C, Zimmermann S, Lambilliotte R, Plassard C, Marmeisse R, Thibaud JB, *et al.*  
622 Molecular and functional characterization of a Na<sup>+</sup>-K<sup>+</sup> transporter from the Trk family in the  
623 ectomycorrhizal fungus *Hebeloma cylindrosporum*. *J. Biol. Chem.* 2007; 282: 26057–26066.
- 624 [63] Heaton LLM, Jones NS, Fricker MD. A mechanistic explanation of the transition to simple  
625 multicellularity in fungi. *Nat Commun.* 2020; 11: 2594. [https://doi.org/10.1038/s41467-020-](https://doi.org/10.1038/s41467-020-16072-4)  
626 [16072-4](https://doi.org/10.1038/s41467-020-16072-4).  
627

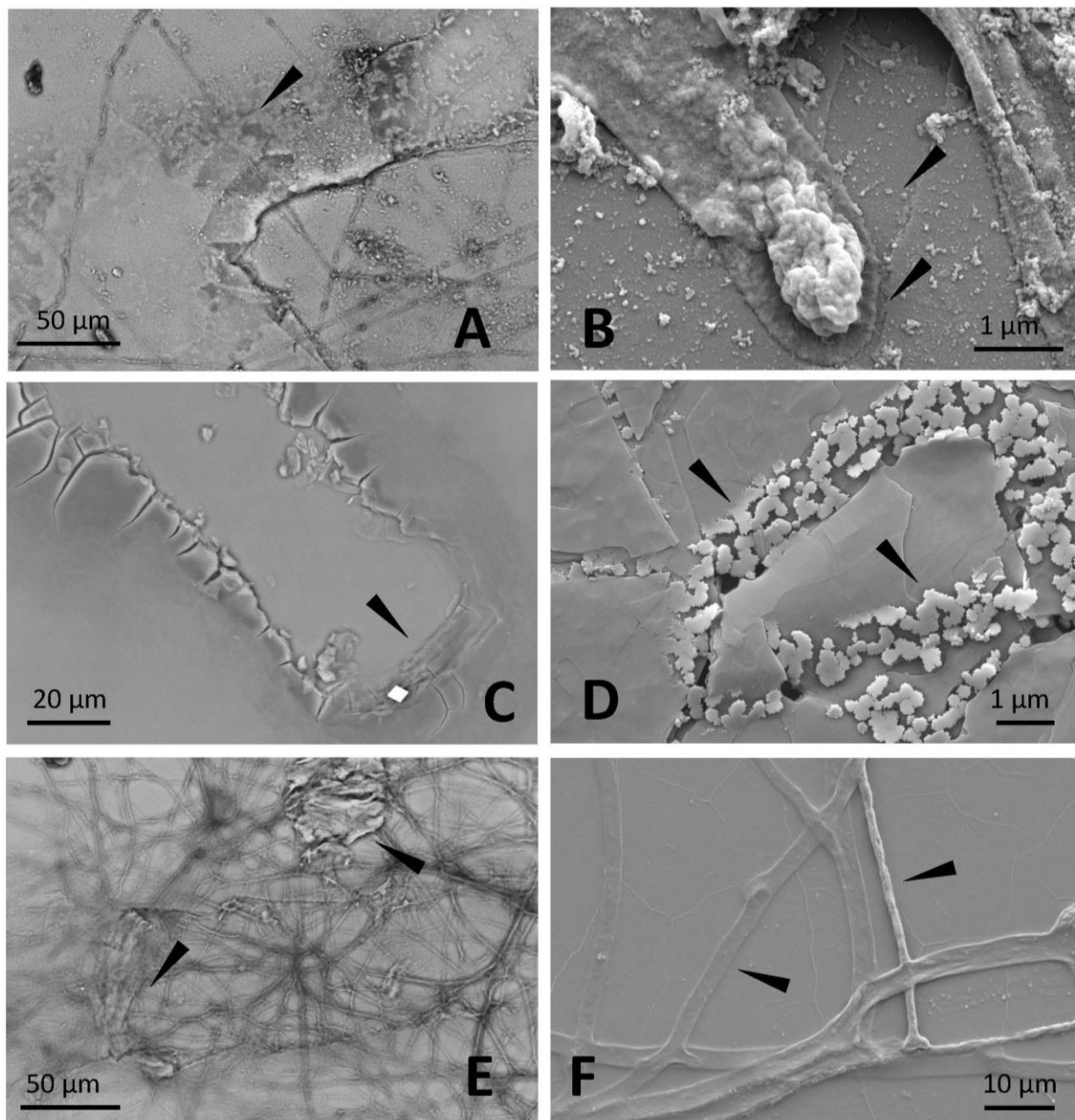
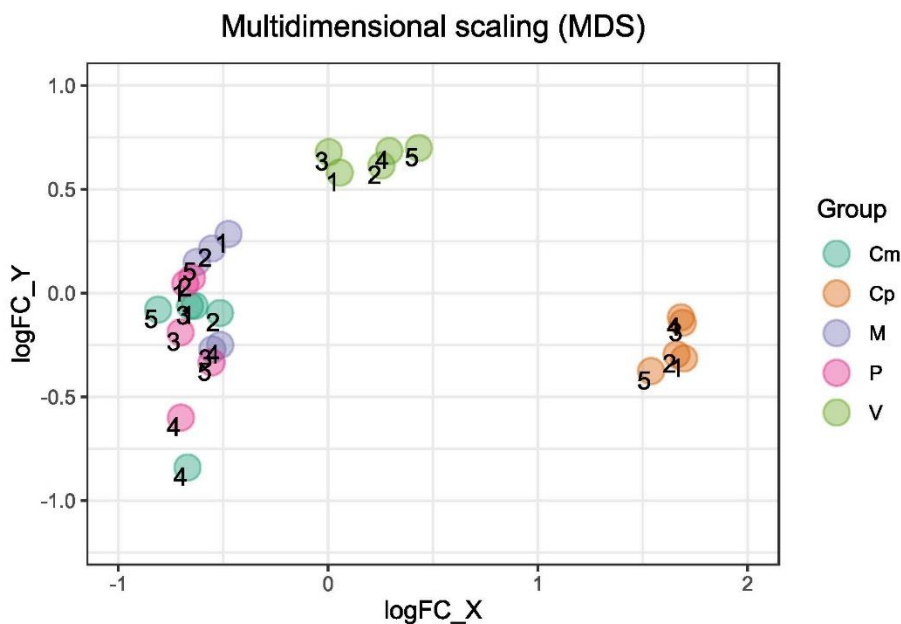
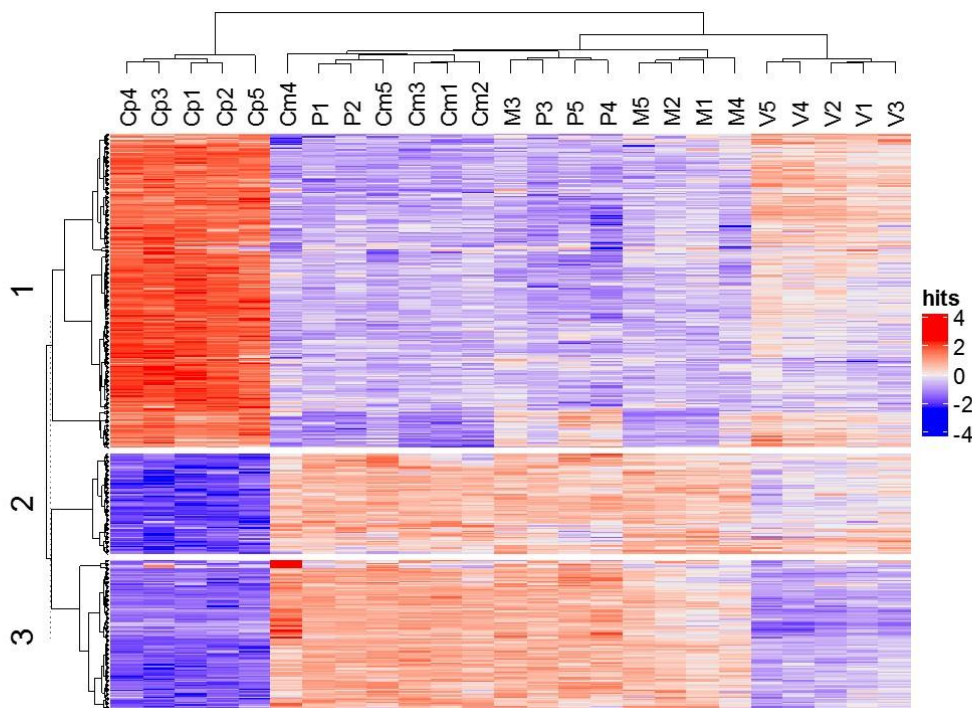


**Figure 1.** Scanning Electron Microscopy imaging of the minerals after fungal growth. On the left (A, C, E), images obtained in variable pressure mode with backscattering detector, on non-coated samples. On the right (B, D, F), images captured in a high vacuum on gold-palladium coated samples. A) muscovite: the arrow indicates superficial erosion of the mineral that occurred after the exposure to fungal activity; B) muscovite: the arrows point to the tip of a fungal hypha attached to the surface of the mineral, and the superficial trenching; C) phlogopite: the arrow points to the edge of a furrow caused on phlogopite surface by the fungus; D) phlogopite: the arrows indicate regular clusters of depositions between the crack caused by the fungus onto the surface of the crystal; E) K-vermiculite: the arrows indicate surface erosion, with a localised scratching and slipping of the surface layer of the crystal; F) K-vermiculite: the arrows indicate fungal hyphae adhering to the mineral's surface, with some flattened, also due to the high vacuum, and others filled with some precipitated material.



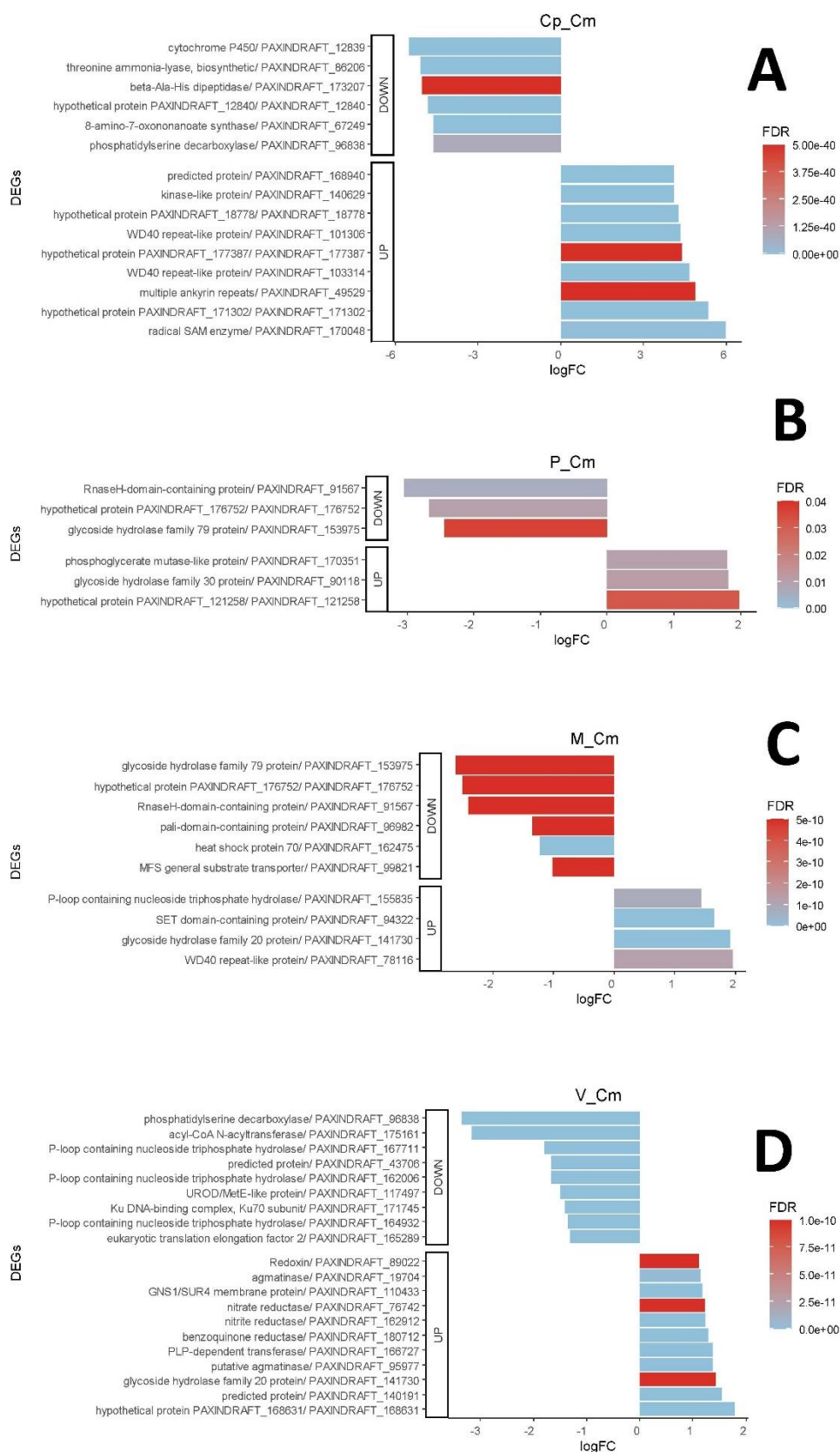
643  
644  
645  
646  
647  
648

**Figure 2.** Multidimensional Scaling analysis of transcriptomes obtained from the *P. involutus* grown K-vermiculite, muscovite and phlogopite as well as positive and negative controls. The distances represent the log<sub>2</sub> fold change between samples. The symbols differentiate between experiments, the numbers represent the biological replicates within each experiment.



649  
650  
651  
652  
653  
654  
655

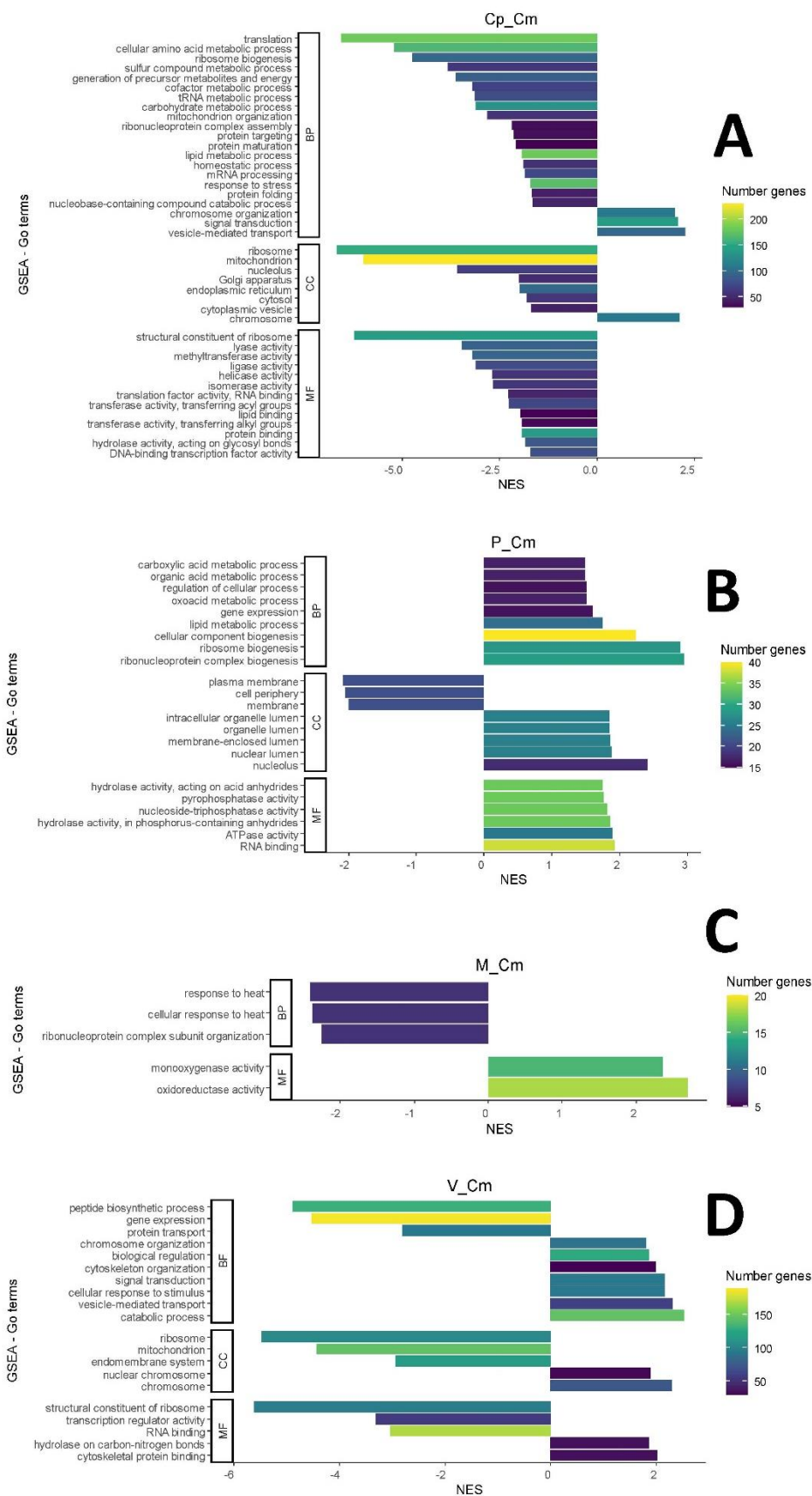
**Figure 3.** Heatmap of the top 1000 differentially expressed genes (ranked by FDR). It is a two-dimensional visual representation of data in which a range of colours represents numerical values of points. The dendrograms added to the left, and top are produced by a hierarchical clustering method based on Euclidean distance computed between the differentially expressed genes (left) and samples (top).



656  
657  
658  
659  
660

**Figure 4.** Top Up- and Down-regulated genes between the experiments in which the fungus grew in the presence of the three minerals (V, P and M) compared to the negative control situation (Cm).





661  
662  
663  
664  
665

**Figure 5.** Gene Set Enrichment Analysis (GSEA). Treatments with the three minerals (V, P and M) and the positive (Cp) control, compared to the negative (Cm) control condition.

666 **Table 1.** Uptake of elements by the fungal mycelium. Values are the means ( $\pm$ SD) from n=5  
 667 replicates. Means in a column without a common letter (a/b/c) differ for P < 0.05, as analysed by one-  
 668 way ANOVA and Tukey's post hoc test.  
 669

	K	Mg	Al	P	Na	Ca	Fe
	<i>ppm (<math>\mu\text{g g}^{-1}</math> of dry mycelium)</i>						
Cp	304.11 $\pm$ 11.05 a	7.16 $\pm$ 0.35 a	0.06 $\pm$ 0.001 b	110.54 $\pm$ 5.70 a	6.55 $\pm$ 0.38 c	3.20 $\pm$ 0.17 a	0.33 $\pm$ 0.04 b
Cm	5.52 $\pm$ 1.69 c	5.82 $\pm$ 0.75 a	0.07 $\pm$ 0.01 b	70.35 $\pm$ 10.49 b	47.76 $\pm$ 11.47 b	2.99 $\pm$ 0.52 ab	0.33 $\pm$ 0.04 b
M	6.80 $\pm$ 0.96 c	6.21 $\pm$ 0.85 a	0.28 $\pm$ 0.09 b	73.24 $\pm$ 11.07 b	51.35 $\pm$ 8.31 b	2.56 $\pm$ 0.41 b	0.48 $\pm$ 0.09 b
P	8.64 $\pm$ 2.91 c	6.67 $\pm$ 1.15 a	1.12 $\pm$ 0.78 a	68.57 $\pm$ 7.90 b	47.64 $\pm$ 8.00 b	2.73 $\pm$ 0.23 ab	0.93 $\pm$ 0.50 a
V	25.11 $\pm$ 4.31 b	6.75 $\pm$ 0.47 a	0.16 $\pm$ 0.04 b	79.52 $\pm$ 4.52 b	64.57 $\pm$ 4.81 a	2.63 $\pm$ 0.23 ab	0.41 $\pm$ 0.06 b
Pr > F (Model)	< 0.0001	0.10	0.0001	< 0.0001	< 0.0001	0.04	0.0001
Significant	Yes	No	Yes	Yes	Yes	Yes	Yes

670

671

672 **Table 2.** Correlation coefficient (Pearson) between elements concentration in the fungal mycelium  
 673 across all the experiments. Values range from -1 (complete negative linear correlation between  
 674 variables) to 1 (complete positive linear correlation).  
 675

Variables	Na	Mg	Al	P	K	Ca	Fe
Na	<b>1</b>	-0.08	0.20	<b>-0.59</b>	<b>-0.87</b>	-0.33	0.22
Mg	-0.08	<b>1</b>	0.39	<b>0.67</b>	<b>0.42</b>	<b>0.54</b>	<b>0.43</b>
Al	0.20	0.39	<b>1</b>	-0.28	-0.28	-0.10	<b>0.99</b>
P	<b>-0.59</b>	<b>0.67</b>	-0.28	<b>1</b>	<b>0.89</b>	<b>0.63</b>	-0.26
K	<b>-0.87</b>	<b>0.42</b>	-0.28	<b>0.89</b>	<b>1</b>	<b>0.49</b>	-0.28
Ca	-0.33	<b>0.54</b>	-0.10	<b>0.63</b>	<b>0.49</b>	<b>1</b>	-0.10
Fe	0.22	<b>0.43</b>	<b>0.99</b>	-0.26	-0.28	-0.10	<b>1</b>

*Values in bold are statistically significant (p<0.05)*

676

677

678

679 **Table 3.** Number of up- and down-regulated genes between pairs of treatments (FDR < 0.05), positive  
 680 control (C plus K= Cp), K-vermiculite (V), phlogopite (P), muscovite (M) and negative control (C  
 681 minus K= Cm). In parenthesis those genes that were up- and down-regulated for more than 2 logFC,  
 682 without parenthesis those genes that were up- and down-regulated for more than 1 logFC. Total DEGs  
 683 is the sum of up and down regulated genes for (FDR < 0.05).  
 684

	Up-regulated	Down-regulated	Total significant DEGs	Total genes shared between pairs of conditions
	Log FC>1 (Log FC>2)	Log FC>-1 (Log FC>-2)		
<b>M/Cm</b>	21 (0)	8 (5)	29	968
<b>P/Cm</b>	39 (1)	8 (5)	47	1335
<b>V/Cm</b>	191 (11)	248 (35)	439	5008
<b>Cp/Cm</b>	832 (111)	676 (155)	1508	7536
<b>M/Cp</b>	583 (103)	744 (120)	1327	7355
<b>P/Cp</b>	730 (103)	891 (120)	1621	7732
<b>V/Cp</b>	198 (39)	428 (62)	626	5786

685